Simulation and experimental results of a new control strategy for point stabilization of nonholonomic mobile robots

Ernesto Fabregas, Gonzalo Farias, Ernesto Aranda-Escolástico, Gonzalo Garcia, Dictino Chaos, Sebastián Dormido-Canto, and Sebastián Dormido

***Abstract*—This work presents a closed-loop position control of a mobile robot, which is capable of moving from its current position to a target point by manipulating its linear and angular velocities. The main objective of this paper is to modify an existing control law based on the kinematic model to improve the response when the robot is backwards oriented and to reach the destination point in less time and with a shorter trajectory. Stability of the proposed control law is validated by Lyapunov Criterion. Some procedures are implemented to test this approach both in simulation with MATLAB, and experimentally with the Khepera IV robot.**

***Index Terms*—Position control; Differential wheeled mobile robots.**

I. INTRODUCTION

ROBOTICS has had a great impact on different fields of daily life during the last years [1], [2]. In this context, mobile robots have become very popular in educational, commercial and social environments. For example, some hospitals have been using autonomous mobile robots for different tasks including delivery services as in [3], [4]. Universities have added robotics laboratories to their engineering curricula with research purposes like in [5], [6]. Warehouses have installed mobile robots to efficiently move materials from stocking shelves to order fulfillment zones [7], [8].

In these kinds of applications, the robot has to navigate in different environments by controlling its own position. The position control of a mobile robot is an experiment where the robot has to reach a target point (T_p) by manipulating its linear and angular velocities (V, ω). The control law obtains these values to reduce the distance and the angle to the T_p under nonholonomic constraints, like in [9]–[12]. Other variables can also be considered in the control law such as the final orientation of the robot (heading orientation).

This maneuver, also known as "point stabilization", has been widely studied during the last years. Different approaches to this problem can be found in the literature. For example, in [13], [14] the authors addressed this problem, and they proposed a variety of position control strategies. In [15] the author makes an exhaustive analysis of the problem and proposes a solution that takes into account the final orientation of the robot, which implies that the trajectory to the goal may not be optimal. In [16] the authors present a control law based on the kinematic model of the robot, which provides the reference speed to the PID control of a DC motor. In [17] the authors present an adaptive position control algorithm of the nonholonomic mobile robot. On the other hand, in [18], [19] the authors present the position control of a robot with obstacles avoidance algorithms based on the potential field method [20] and their limitations. This solution has been used by the authors of the present paper in different previous works [21]–[23]. After multiple tests, experimentation and studies, two main limitations have been detected in this control law: 1) when the robot is far away from the T_p, the linear velocity is maximum, which means that the robot cannot turn as fast as possible; and 2) when the angular error is large, the angular velocity ω takes undesirable values. Some control laws (see e.g. [11], [16]) avoid this issue simply allowing the robot to move backwards. However, this capability is not available in all the devices, and even when it is possible, the robot needs additional sensors to avoid obstacles while moving backwards. Other papers propose complex strategies such as adaptive [17] or predictive controllers [24], however they do not take into account saturation in the velocities, which also hinders its implementation. Therefore, the objective is to improve the control law in [19] to obtain an alternative to the methods in the literature, which is realistically and easily implementable with a good performance.

Following this idea, in [25] we proposed a preliminary control law, by modifying the angular velocity expression of [19]. In this paper, we improve the control law in [25]

Manuscript received Month xx, 2xxx; revised Month xx, xxxx; accepted Month x, xxxx. This work was supported in part by the Spanish Ministry of Economy and Competitiveness under the Projects No. DPI2017-84259-C2-1-R, DPI2017-84259-C2-2-R and ENE2015-64914-C3-2-R, the Spanish Ministry of Science, Innovation and Universities under the Project No. RTI2018-094665-B-I00, and the Chilean Ministry of Education under the Project FONDECYT 1191188.

E. Fabregas, D. Chaos, S. Dormido-Canto and S. Dormido are with the Departamento de Informática y Automática, Universidad Nacional de Educación a Distancia (UNED), Juan del Rosal, 16, 28040. Madrid, Spain. (e-mails: efabregas@bec.uned.es; {dchaos,sebas,sdormido}@dia.uned.es).

G. Farias is with the Escuela de Ingeniería Eléctrica, Pontificia Universidad Católica de Valparaíso (PUCV), Avenida Brasil 2147, Valparaíso, 2362804, Chile. (e-mail: gonzalo.farias@pucv.cl).

E. Aranda-Escolástico is with Department of Informatics, ceiA3, CIESOL, University of Almería (UAL), Ctra. de Sacramento s/n. 04120 La Cañada de San Urbano, Almería, Spain. (e-mail: eaescolastico@gmail.com).

G. Garcia is with the Ocean and Mechanical Engineering, Florida Atlantic University (FAU), Boca Raton, FL 33431, USA. (e-mail: garciag@fau.edu).

modifying the expression of the linear velocity, which enables the robot to reach the T_p in a more efficient way with a smooth trajectory. In addition, theoretical and experimental results are provided. On one hand, a stability analysis is performed using the Lyapunov criterion to guarantee the global asymptotic stability of the system. On the other hand, tests and results of the new implementation in simulation (MATLAB) and experimental demonstrations with Khepera IV robot that validates the proposed theory.

The remainder of the paper is organized as follows. Section II describes the kinematic model of the differential wheeled robot and its position control experiment. Section III shows the existing control law and the proposed solution validated using the Lyapunov stability analysis. Section IV shows the results obtained with the proposed control law in simulation. Section V shows the experimental results obtained with the Khepera IV robot in the laboratory. Finally, Section VI presents the main conclusions and the future works.

II. Model of the Robot and Position Control

A. Kinematic Model of the Robot

A differential wheeled robot is a mobile robot whose movement is based on two separately driven wheels placed on each side of its body. The two drive velocities (V_L, V_R) are perpendicular vectors to the wheels axis. Furthermore, the wheels are assumed to roll without slipping. These conditions impose some restrictions known as nonholonomic constraints [10], [26], [27]. The robot can change its direction by varying the relative rotation between the wheels, so it does not need an additional steering movement to turn. The kinematic model of the robot can be obtained in cartesian coordinates like in [13]–[15], [28].

$$\begin{cases} \dot{x}_c = V\cos(\theta) \\ \dot{y}_c = V\sin(\theta) \\ \dot{\theta} = \omega, \end{cases} \tag{1}$$

where θ is the heading direction angle of the robot and it is perpendicular to the turning radius (R). The instant linear velocity $V = (V_L + V_R)/2$ is the average of the linear velocities of the left and right wheels, V_L and V_R, respectively. The angular velocity $\omega = (V_L - V_R)/l$ is defined with respect to the *ICC (Instantaneous Center of Curvature)*, where l is the distance between the wheels. Naturally, the mobile robot has a maximum linear velocity $V_{\max}$ and, usually, also a minimum turning radius $R_{\min}$, i.e, it cannot freely rotate. Hence, in these cases there exist a maximum angular velocity $\omega_{\max} = V_{\max}/R_{\min}$.

B. Position Control or “Point Stabilization” Problem

The problem of stabilizing the position of a differential wheeled mobile robot in a given $T_p(x_p, y_p)$, irrespective of its orientation, is named position control or point stabilization. The objective is to calculate the velocities of the robot (V,ω) to drive it from the current position $C(x_c, y_c)$ and orientation (θ) to the T_p.

The problem has been widely studied mainly due to the control law design restrictions under nonholonomic constraints, introducing challenging nonlinear control problems from an academic point of view, as the authors presented in [24]. Figure 1 shows the variables involved in this experiment.

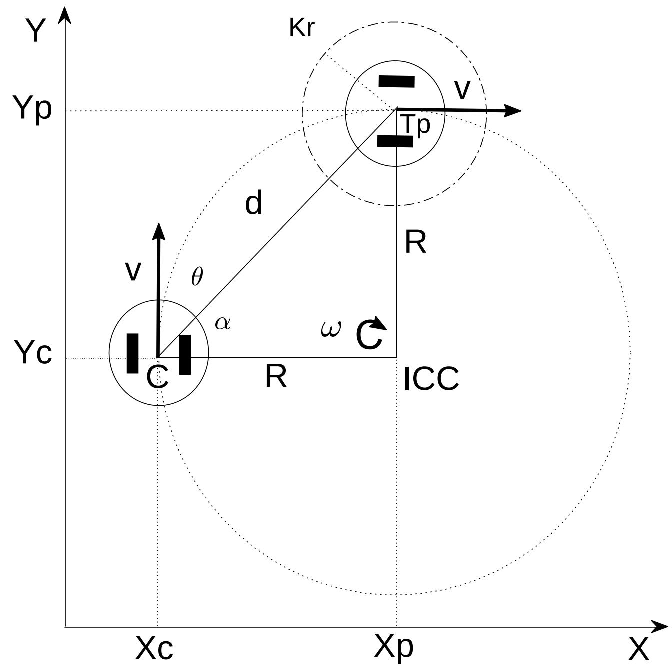

Fig. 1. Involved variables in the position control problem

In order to achieve the control objective, the distance d and the angle α between points C and T_p are obtained as follows

$$d = \sqrt{(y_p - y_c)^2 + (x_p - x_c)^2} \tag{2}$$

$$\alpha = \text{atan2}\left(y_p - y_c, x_p - x_c\right), \tag{3}$$

where atan2(y, x) is the four quadrant arc-tangent of y and x. Equations (2)-(3) imply that $y_p - y_c = d\sin(\alpha)$ and $x_p - x_c = d\cos(\alpha)$. Then, we can define an orientation error

$$e_\theta = \text{atan2}\left(\sin\left(\alpha - \theta\right), \cos\left(\alpha - \theta\right)\right), \tag{4}$$

such that $e_\theta \in [-\pi, \pi]$ is equivalent to $\alpha - \theta$ but lies in the interval $e_\theta \in [-\pi, \pi]$. Now, taking the time derivative of (2) and replacing (1), we obtain

$$\begin{aligned} \dot{d} &= -\frac{\dot{y}_c(y_p - y_c) + \dot{x}_c(x_p - x_c)}{d} = \\ &= -V\left(\sin(\alpha)\sin(\theta) + \cos(\alpha)\cos(\theta)\right) \\ &= -V\cos(\alpha - \theta). \end{aligned}$$

From (4),

$$\begin{aligned} \dot{e}_\theta &= \dot{\alpha} - \dot{\theta} \\ &= \frac{(y_p - y_c)\dot{x}_c - (x_p - x_c)\dot{y}_c}{d^2} - \omega \\ &= \frac{V\sin(\alpha - \theta)}{d} - \omega \end{aligned}$$

Therefore, the following dynamical system is obtained

$$\begin{aligned} \dot{d} &= -V\cos(e_\theta) \\ \dot{e}_\theta &= \tfrac{V}{d}\sin(e_\theta) - \omega. \end{aligned} \tag{5}$$

Consequently, the problem of positioning the mobile robot is solved if it is possible to achieve $d \rightarrow 0$, while V and ω remain bounded.

Figure 2 shows the control blocks diagram of this problem. The robot tries to minimize e_θ, and at the same time, reduce the distance to the T_p ($d = 0$). The values of d and α are calculated in the block *Compute*, using the T_p as the reference and the current position of the robot (*C*). These two values and the orientation θ are used by the *Control Law* block to obtain the control signals (V and ω). It is important to notice that in order to apply this control actions to the robot it is necessary that $|\omega| \leq \omega_{max}$ and $|V| \leq V_{max}$.

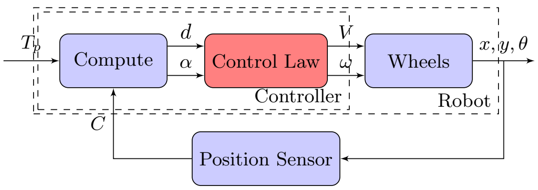

Fig. 2. Diagram of the position control problem

Different solutions for this problem can be found in the bibliography, [15], [16], [29], and [19]. The last one is represented by

$$V = \begin{cases} V_{\max} & \text{if } d > K_r \\ d\left(\frac{V_{\max}}{K_r}\right) & \text{if } d \leq K_r \end{cases} \tag{6}$$

$$\omega = \omega_{\max} \sin\left(e_\theta\right), \tag{7}$$

where the linear velocity V is obtained depending on the distance to the T_p. When the robot is far from the T_p, V is saturated to $V_{\max}$. This velocity decreases when the robot enters into the docking area, being K_r the radius of a docking area around the T_p (see Fig. 1). At the same time, ω is obtained as a function of the orientation error to the T_p (e_θ) in order to overcome the term $\frac{V}{d}\sin(e_\theta)$ in (5).

III. Proposed Control Law and Stability

A. Control law modifications

In the control law of [19], the linear velocity V is a function of the distance to the T_p and it is saturated for large values of it. This implies that it is maximum when the robot is far from the target (out of the docking area), even when it is not correctly oriented. In these situations, the robot might take some time to reach the orientation to the T_p and during this time it will get further away from the T_p.

When the robot is far from the T_p and the orientation error is big, it is more desirable for the robot to reach the correct orientation first instead of making the linear velocity to reach its maximum value at the beginning. That is why we propose for these situations to relate the linear velocity to the orientation error. This modification can grant that the linear velocity be dismissed depending on the orientation error to facilitate an increase in the angular velocity. Therefore, the proposed linear velocity becomes

$$V = \min\left\{K_1 d p\left(e_\theta\right), V_{\max}\right\}, \tag{8}$$

where

$$p\left(x\right) = \left(\frac{\pi - |x|}{\pi}\right) \tag{9}$$

which satisfies $0 \leq p(x) \leq 1$ for $x \in [-\pi, \pi]$. Notice that due to (4), e_θ is normalized to the interval $\in [-\pi, \pi]$ thus $0 \leq p(e_\theta) \leq 1$.

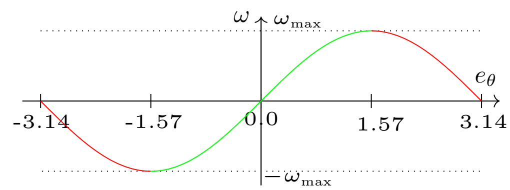

Fig. 3. Value of ω vs. e_θ

The previous control law presented in 6 and (7) grants the range of the angular velocity between $-\omega_{\max} \leq \omega \leq \omega_{\max}$ but it has an unwanted behavior for values of $|e_\theta| \geq \frac{\pi}{2}$ (see Figure 3). In this region, the relation between ω and the error angle is inverse ($|\omega|$ decreases when the $|e_\theta|$ increases).

As a result of this behavior, when the T_p is at the back of the robot, ω can be very small, as if the robot were almost oriented to the target. Furthermore, when the angle error is $e_\theta = \pm 180°$ (green line), the $\sin(e_\theta) = 0$ and then, $\omega = 0$, and the robot starts moving away from the T_p without turning. This is because, for the control law, the T_p is wrongly aligned in front of the robot, when in fact the T_p is behind the robot. To mitigate this behavior, it is proposed in this paper to add Integral Action to this control law to improve the speed of change of the angular velocity especially in these situations. Besides, the term $\omega_{\max}$ is substituted by a K_p term to control the Proportional Action in relation to the Integral Action.

$$\omega(t) = K_p \sin\left(e_\theta(t)\right) + K_i \int_0^t e_\theta(s) ds \tag{10}$$

In addition, parameters K_1, K_p and $K_i > 0$ are chosen to satisfy the following constraints

$$0 < K_1 < K_p \tag{11}$$

$$K_p + \sqrt{K_i}\pi < \omega_{\max}. \tag{12}$$

B. Stability Analysis

The stability of the system is assessed by using the Lyapunov theory based on [16], [30]–[32]. Firstly, let us consider an auxiliary state $z = \int_0^t e_\theta(s) ds$ such that the system to be controlled becomes

$$\begin{aligned} \dot{d} &= -V\cos(e_\theta) \\ \dot{e}_\theta &= \tfrac{V}{d}\sin(e_\theta) - \omega \\ \dot{z} &= e_\theta. \end{aligned} \tag{13}$$

From solving (13) in steady state condition, it is obtained that $\dot{z} = e_\theta = 0$, which implies $\dot{d} = -K_1 d = 0$ and $\dot{e}_\theta = K_i z = 0$, and, consequently, a single equilibrium point is defined, the origin $(0, 0, 0)$. This point is used for stability analysis and asymptotic convergence testing. First, let us consider the following proposition.

Proposition 1. *Consider a system $\dot{x}(t) = f(t,x)$ and suppose $f(t,x)$ is piecewise continuous in t and locally Lipschitz in x, uniformly in t, on $[0,\infty) \times \mathbb{R}^n$. Furthermore, suppose $f(t,0)$ is uniformly bounded for all $t \geq 0$. Let $\mathcal{L} : \mathbb{R}^n \to \mathbb{R}$ be a continuous positive definite differentiable function such that $\dot{\mathcal{L}}(x(t)) \leq W(x)$, $\forall t \geq 0$, $\forall x \in \mathbb{R}^n$, where $W(x)$ is a continuous positive semidefinite function. Then, $W(x(t)) \to 0$ as $t \to \infty$.*

Proof. This proposition can be obtained from Theorem 8.4 in [33] doing $D = \mathbb{R}^n$ and $W_1 = W_2 = \mathcal{L}$. □

Now, the following theorem can be stated.

Theorem 1. *The dynamical system* (13) *under the control laws* (8) *and* (10) *satisfying constrains* (11) *and* (12) *is globally asymptotically stable.*

Proof. Replacing (8) and (10) in (13), we obtain

$$\dot{d} = -\min\left\{K_1 dp\left(e_\theta\right), V_{\max}\right\}\cos(e_\theta) \tag{14a}$$

$$\dot{e}_\theta = \frac{\min\left\{K_1 dp\left(e_\theta\right), V_{\max}\right\}}{d}\sin(e_\theta) - K_p \sin\left(e_\theta(t)\right) - K_i z \tag{14b}$$

$$\dot{z} = e_\theta. \tag{14c}$$

In order to analyze the stability, we consider first the subsystem (14b)-(14c) with states e_θ and z and input $d(t)$. Then, the following the Lyapunov function is selected

$$\mathcal{L}_1 = \frac{e_\theta^2}{2} + \frac{K_i z^2}{2}. \tag{15}$$

If we assume first that $\omega < \omega_{\max}$, then the control law is feasible and its time derivative becomes

$$\begin{aligned}\dot{\mathcal{L}}_1 &= e_\theta\left(\frac{\min\left\{K_1 dp\left(e_\theta\right), V_{\max}\right\}}{d}\sin(e_\theta) - K_p\sin(e_\theta)\right) \\ &\leq \left(K_1 p\left(e_\theta\right) - K_p\right)\sin(e_\theta)e_\theta = W(e_\theta)\end{aligned} \tag{16}$$

As $0 \leq p\left(e_\theta\right) \leq 1$ for $-\pi \leq e_\theta \leq \pi$, it is clear that condition (11) guarantees that $W(e_\theta) \geq 0$. In addition, if $e_\theta = z = 0$, then $\dot{e}_\theta = \dot{z} = 0$, and from Proposition 1 it follows that $W(e_\theta(t)) \to 0$ as $t \to \infty$. To analyze asymptotic stability notice that $W(e_\theta) = 0$ for $e_\theta = 0, \pm\pi$. If e_θ tends to $\pm\pi$, then z tends to $\pm\infty$ by (14c), but then $\mathcal{L}$ tends also to ∞, contradicting (16). Hence, the only possibility is $e_\theta \to 0$.

Now, by Barbalat's Lemma [33], as $\int_0^t \dot{e}_\theta(t)dt = 0 - e_\theta(0)$ exists and is finite, then $\dot{e}_\theta \to 0$, and using (14b), $z \to 0$ is obtained. Thus, the subsystem is globally asymptotically stable. Next, we have to prove the initial assumption, i.e, that the angular velocity cannot be saturated. From (10) and (12) we know that $|\omega(0)| = |K_p \sin\left(e_\theta(0)\right)| \leq K_p \leq \omega_{max}$. Consequently, the angular velocity is not saturated in the initial time. In addition, by its definition, the initial integral error is zero, i.e, $z(0) = 0$. Hence, $\mathcal{L}_1(0) \leq \frac{\pi^2}{2}$.

Let us now suppose that ω saturates, then there must exist a time t_1 such that $|\omega(t_1)| = \omega_{\max}$. Since $\mathcal{L}_1$ cannot decrease while $t \in [0, t_1)$ because $|\omega| \leq \omega_{\text{sat}}$ is not saturated, we have $\mathcal{L}_1(t_1) \leq \mathcal{L}_1(0)$, so

$$\frac{e_\theta^2(t_1)}{2} + \frac{K_i z^2}{2} \leq \mathcal{L}_1(0) \to \frac{K_i}{2}z^2 \leq \mathcal{L}_1(0) \leq \frac{\pi^2}{2}.$$

Therefore $|z(t_1)| \leq \pi/\sqrt{K_i}$. But if $|z(t_1)| \leq \pi/\sqrt{K_i}$, then $|\omega(t_1)| \leq K_p + \sqrt{K_i}\pi$ and due to condition (12), $\omega(t_1) < \omega_{\max}$. Thus this contradicts our initial assumption and therefore the angular velocity never saturates.

We then conclude that $e_\theta, z \to 0$ as $t \to \infty$. Furthermore there exist a time T such that $|e_\theta(t)| < \pi/3$ for $t > T$. Now, let's consider the subsystem (14a) with state d and input e_θ. First, note that T is, in fact, a monotonically increasing function of $e_\theta(0)$, and that $\dot{d}$ is bounded by $V_{\max}$. Hence, $d(t)$ is bounded by $d(t) < d(0) + V_{\max}T$ for all t, because for $t > T$ it is going to be shown that $d(t)$ decreases. Using this inequality and that $\mathcal{L}_1(t) \leq \mathcal{L}_1(0)$, we know that $|e_\theta(t)| \leq \sqrt{2\mathcal{L}_1(0)}$ and $|z(t)| \leq \sqrt{2\mathcal{L}_1(0)/K_i}$, thus we can conclude that

$$||\left[d, e_\theta, z\right]|| \leq \sqrt{2\mathcal{L}_1(0)}\left(1 + \frac{1}{\sqrt{K_i}}\right) + d(0) + V_{\max}T(e_\theta(0)).$$

So, the state remains in a neighborhood of the origin and is stable in the Lyapunov sense. Finally, we prove that, for $t > T$, $d(t) \to 0$ when $t \to \infty$ and the system is globally asymptotically stable. After T, it is satisfied that $|e_\theta(t)| < \pi/3$. This implies that $1/2 < \cos(e_\theta) \leq 1$ and that $2/3 < p(e_\theta) \leq 1$. Then we propose the following Lyapunov function

$$\mathcal{L}_2 = \frac{d^2}{2} \tag{17}$$

Its time rate of change is then

$$\begin{aligned}\dot{\mathcal{L}}_2 &= -d\min\left\{K_1 dp\left(e_\theta\right), V_{\max}\right\}\cos(e_\theta) \\ &\leq -\frac{d}{2}\min\left\{\frac{2}{3}K_1 d, V_{\max}\right\}\end{aligned} \tag{18}$$

which is negative definite since by definition $d \geq 0$, thus, by Proposition 1, $d \to 0$ as $t \to \infty$. □

Remark: Note that despite of $e_\theta \to 0$, it is not implied that the mobile robot must finish with a prefixed or desired orientation. This enables the avoidance of the constraints of Brockett's Theorem [34] and obtaining a continuous control law. In order to illustrate the behaviour of the control law this

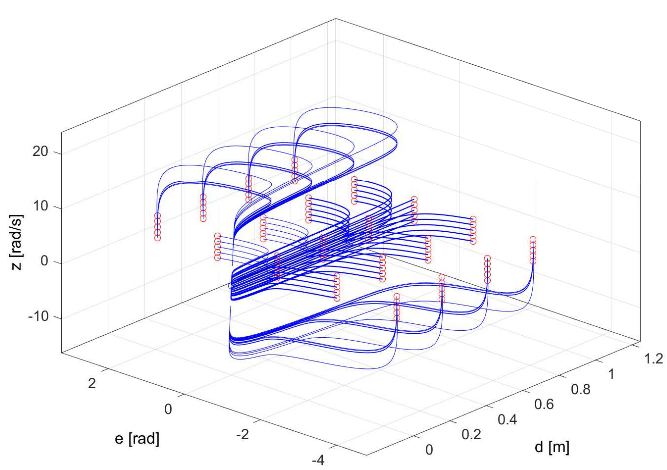

Fig. 4. $3D$ Phase Portrait with a Dense Grid of Initial Conditions: $e : \{-\pi, -\pi/2, 0, \pi/2, \pi\}$, $d : \{0.25, 0.5, 0.75, 1\}$, and $z : \{-2, -1, 0, 1, 2\}$ and with parameters $K_1 = 0.1$, $K_p = 1.4$, and $K_i = 0.008$.

Subsection also includes a $3D$ phase portrait graph asserting the results obtained from the Lyapunov analysis. Phase portrait is a useful graphical aid for stability assessment for low order systems. Figure 4 shows a $3D$ phase portrait with trajectories for the system (15) starting from different initial conditions (from an equally spaced grid of initial condition points). This figure shows that the propagation of all chosen trajectories converges always to the origin.

IV. Simulation Results

In this section, some results obtained in simulation using MATLAB are discussed. First, the previously described problems of the existing control law are showed. Then, the results of the experiment with the proposed control law are compared with it.

Figure 5 shows the results of the previous control law [19] for different initial conditions to represent the special case of $e_\theta = \pm 180°$. The initial position of the robot is (0;0) and the T_p (1;1). It means that the angle between the initial position of the robot and the T_p is $\alpha = 45°$. The color lines show the described trajectories of the existing control law (Villela) for different initial orientation angles ($\theta = 0°$, $-45°$, $-90°$,...,$-90°$). The special case occurs when $\theta = -135°$ (green color line), which means that the error is $e_\theta = 45° - (-135°) = 180°$. In this case, the angular velocity is $\omega = 0.0$ because $sin(180°) = 0$. That is because for this value the robot does not turn, as can be observed.

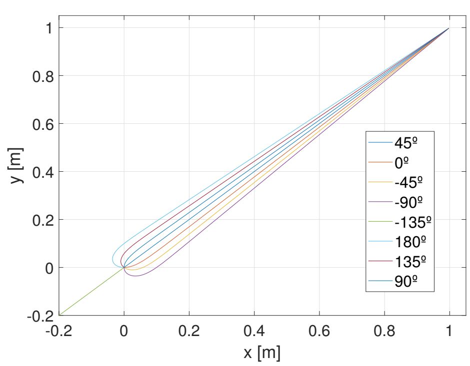

Fig. 5. Position control of the robot for different initial orientations.

Figure 6 shows the implementation of the new control law with similar conditions from the previous experiment for the special case of an initial orientation ($\theta = -135°$ and $e_\theta = 180°$). The lines represent the trajectories of the robot to reach the T_p for different values of $K_i = (0.000, 0.0022, 0.0045, ..., 0.158)$ and $K_p = 1.4$ in equation (10). These values are chosen to be a representative sample of K_i in order to obtain a correct visualization. Note also that the controller is robust enough to admit K_i larger than the value imposed in equation (12). Observe that a smaller K_i implies a wider turn but then the mobile robot reaches the target following a straight line. However, a larger K_i produces a sharp first turn but also larger overshoot.

As it is shown for $K_i = 0.0$ the behavior is the same of the control law of [19] because the Integral Action is not actuating, while for some of the remaining values, the behavior

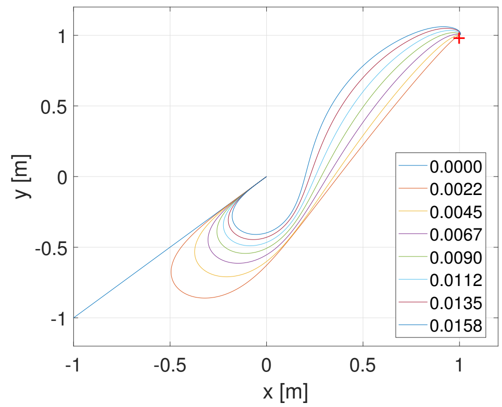

Fig. 6. Special case of $e_\theta = 180°$ for different values of K_i.

of the trajectory is improved. These parameters can be adjusted taking into account a trade-off between distance and energy consumption of the trajectory.

Figure 7 shows the position of the robot in the x-y plane [m] for both cases: the previous control law (blue line) and the proposed control law (brown line). The parameters used for these experiments are the following: $v_{\max} = 0.05$ m/s, $\omega_{\max} = 0.7853$ rad/s, $K_r = 0.025$ m, $K_p = 0.75$, $K_1 = 0.1$ and $K_i = 0.00007$. The initial position of the robot for both experiments is point $C(-0.4; 0.0)$. The orientation $\theta = -178°$ and the T_p is marked at $T_p(0.8; 0.0)$. As it can be observed, with the proposed control law the robot describes a shorter path to the T_p. Note that these parameters are taken from the *Khepera IV* robot, which is going to be used later for experimental testing.

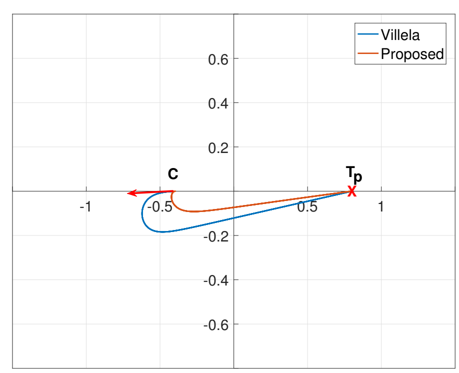

Fig. 7. Control law [19] vs. proposed: xy plane

Figure 8 shows the distance of the robot to the T_p vs. time. As it can be observed, with the proposed control law the robot reaches the T_p in less time (around 4 seconds) than with the previous one. This is because with the previous control law, at the beginning of the path, the distance to the goal is increased, due to the robot taking longer to turn to the desired orientation (T_p).

Figure 9 shows the values of linear velocity [m/s] vs. time [s] for both algorithms. The blue line represents the previous control law and the brown line represents the proposed one. As it can be observed, in the proposed control law the linear

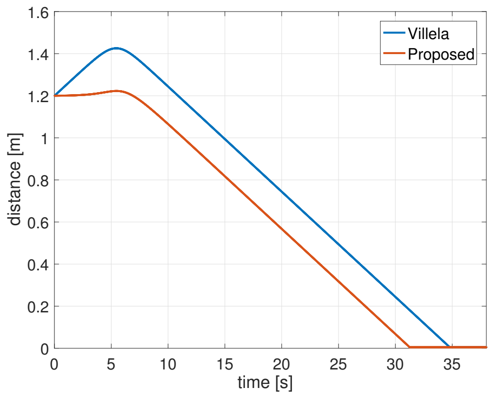

Fig. 8. Control law [19] vs. proposed: distance vs. time

velocity at the beginning is $v = 0.0m/s$ and it starts to increase. In contrast, for the previous control law, the linear velocity at the beginning is the maximum ($v = 0.05m/s$). This implies that in the proposed control law when the orientation error to the T_p is big enough, the angular velocity is more important than linear velocity. In other words, it is more important to turn than to move forward in order to reach the desired orientation as soon as possible. If the robot is not well oriented, what it does initially is move away from the T_p.

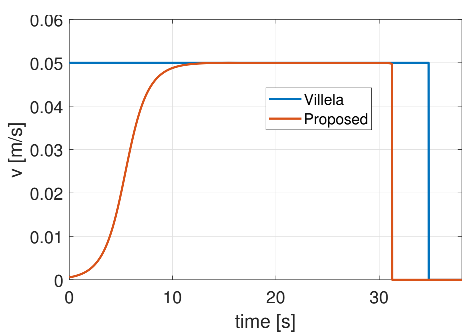

Fig. 9. Control law [19] vs. proposed: linear velocity vs. time

Figure 10 shows the angular velocity of both control laws for the same experiment. As can be seen in both cases the maximum value of the angular velocity is reached almost at the same time instant ($t \approx 7s$). In the case of the proposed control law, the linear velocity starts from 0, which allows the robot to turn more than advance to reach the orientation to the T_p first and follow a shorter path to the target.

Figure 11 shows a simulation for the comparison between the three involved control laws for the special case of an initial orientation ($e_\theta = 180°$). The red arrow indicates the initial orientation of the robot at the starting point (C). The red cross indicates the T_p. The blue line (Villela) represents the control law in [19], which presents the limitation explained in figure 5 for these initial conditions. The yellow line (PID'18) represents the control law that we proposed before in [25] to avoid this limitation. The orange line (Proposed) represents the proposed control law in the present work, which is an improvement to the previous control law that we proposed (PID'18). As it can be seen, in this case for this initial

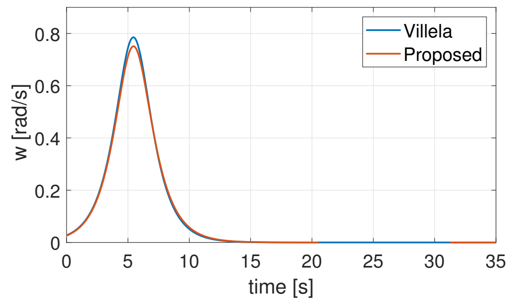

Fig. 10. Control law [19] vs. proposed: angular velocity vs. time

conditions, the robot reaches the T_p with a shorter trajectory and in less time.

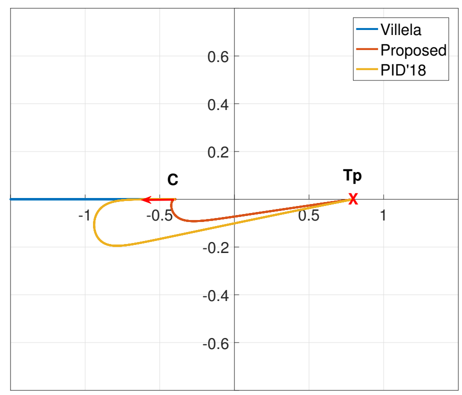

Fig. 11. Comparison between the involved control laws: xy plane [m]

To show the differences between the two methods in a better way, we have compared different performance indexes shown in Table I. We can observe that the proposed method provides an improvement in the performance of the system since it is able to bring the robot faster to the T_p. Consequently, the different measurements of the integral error of the position over time are reduced.

TABLE I
COMPARISON BETWEEN THE CONTROLLER IN [19] AND THE PROPOSED CONTROLLER IN SIMULATION

Index	Villela	Proposed	Improvement
IAE	28.87	23.28	19.34%
ISE	30.77	22.18	27.91%
ITAE	351.46	255.00	27.44 %
ITSE	299.35	192.94	35.55 %

V. EXPERIMENTAL RESULTS

In this section, some experimental results with a platform in the laboratory are shown to validate the results of the new control law. This platform is similar to the presented by the authors in [23], [35]. It has been developed by the authors to perform position and formation control experiments with Khepera IV robots and a WI-FI network. The platform provides the absolute position of the robots with an indoor positioning system (IPS). The main components of the IPS are an overhead camera that obtains an image of the workspace. This image is processed in a PC with Swistrack software tool, which obtains the position and orientation of the robot in real time. The position and orientation are sent to the robot thought the WI-FI network.

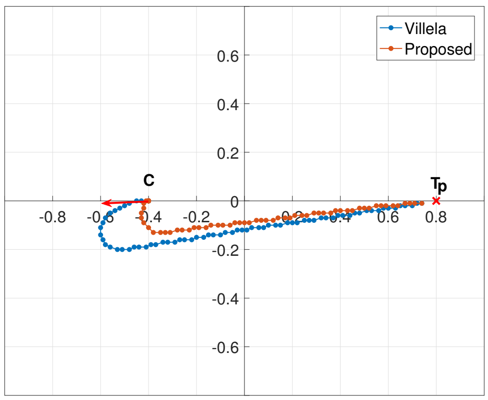

Fig. 12. Control law [19] vs. proposed: xy plane [m]

Figure 12 shows the position control experiment similar to Figure 7, but in this case with the platform in the lab. The blue line represents the previous control law (Villela), and the brown line represents the proposed control law. The initial conditions are similar to the experiment in simulation time. The start point is $C(-0.4; 0.0)$, the initial orientation is represented by the arrow with a value of $\theta = -178°$ and the target point is marked at $T_p(0.8; 0.0)$ with a red X. As it can be observed, the behavior of the robot is the same as the one obtained in simulation time for the same initial conditions. The proposed control law has better performance and the robot reaches the T_p with a more direct trajectory. Due to the modifications introduced to the existing control law.

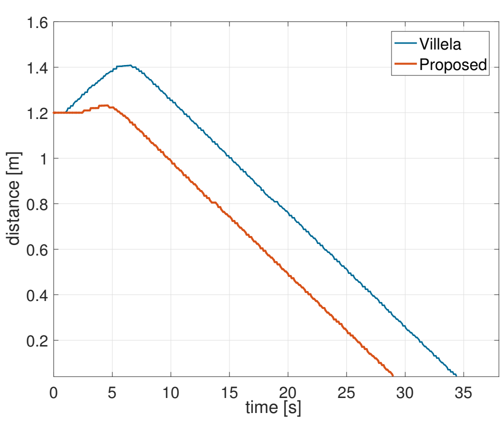

Fig. 13. Control law [19] vs. proposed: distance vs. time

Figure 13 shows the values of the distance for this experiment. The blue line represents the existing control law and the brown line the proposed control law. As it can be observed, the results are similar to the simulation experiment, as expected. In this case, with the proposed control law, the robot reaches the T_p in 5 seconds less than the existing control law. The difference may be due to the friction of the wheels with the surface and the delay in image processing and communications, things that are not taken into account in the simulation. However, the results can be considered very acceptable. Because the improvement with respect to the existing control law is relevant.

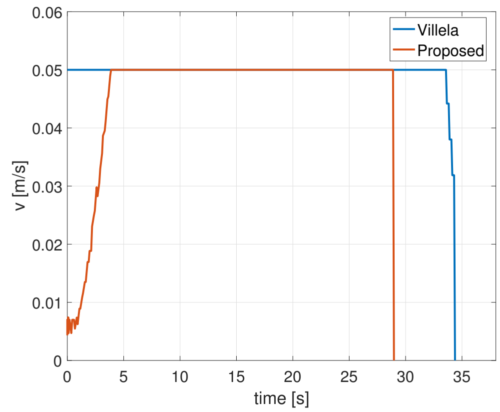

Fig. 14. Control law of [19] vs. proposed: linear velocity vs. time

Figure 14 shows the values of linear velocities of the robot, the same experiment of Figure 13. As can be seen, the linear velocity of the proposed control law starts at small values because it depends on the orientation error to the T_p. This grant that the robot can turn faster to get the correct orientation. After the orientation error is minimized, this velocity is saturated like in the previous control law. When the robot reaches the T_p it stops, which means that the velocity falls to zero. This also shows that the robot reaches the T_p before with the proposed control law.

Figure 15 shows the angular velocity for this experiment and both control laws. As can be seen, the behavior is similar to the results of the simulation. In this case, for the proposed control law, the angular velocity reaches its highest value earlier than previous control law. This means that the robot turns before and reaches the T_p with a shorter path.

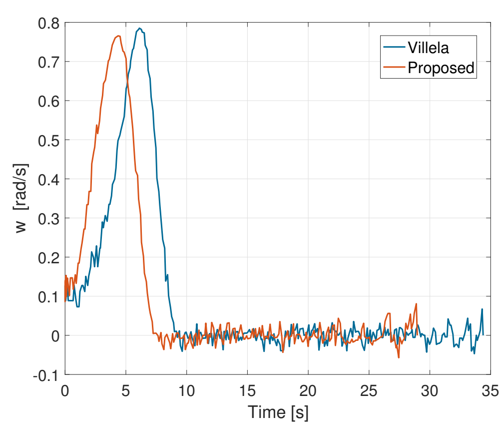

Fig. 15. Control law [19] vs. proposed: angular velocity vs. time

Table II shows different performance indexes of the robot position error for both methods. As can be observed, the improvement is significant for all indexes. In all cases, the values are reduced, similar to the simulation results.

TABLE II
COMPARISON BETWEEN THE CONTROLLER IN [19] AND THE PROPOSED CONTROLLER IN THE EXPERIMENTAL ENVIRONMENT

Index	Villela [19]	Proposed	Improvement
IAE	28.98	21.41	26.14%
ISE	30.67	19.99	34.81%
ITAE	357.52	219.15	38.70%
ITSE	305.72	160.76	47.42%

Finally, to further validate the proposed control law in an experimental environment, eight target points have been selected. Figure 16 shows the trajectories described by the robot for different situations. The initial position for all the cases is $(0.0; 0.0)$ and the orientation is $-180°$. The target points are the following: $1(0.0; 0.5)$, $2(0.5; 0.5)$, $3(0.0; 0.5)$, $4(-0.5; 0.5)$, $5(-0.5; 0.0)$, $6(-0.5; -0.5)$, $7(0.0; -0.5)$ and $8(0.5; -0.5)$. These conditions have been selected thinking in situations of certain difficulty that the control law has to face and solve. For example, the target points were located at different quadrants. As can be seen, in all cases the robot reaches the T_p following a smooth trajectory. These results show that the control law has good performance for different conditions.

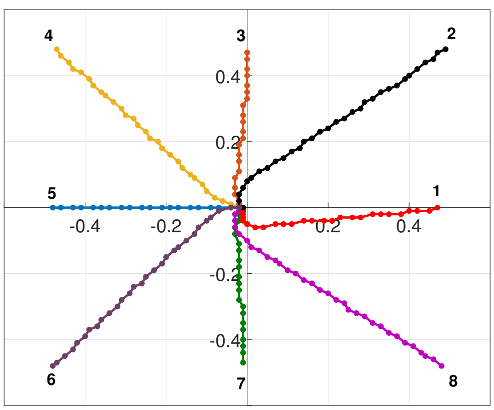

Fig. 16. Results of the position control with the proposed control law

VI. CONCLUSION

This paper presents a new control law to drive a mobile robot from its current position to a T_p. These kinds of control laws manipulate the angular and linear velocities of the robot. The proposed control law implements two main improvements to an existing control law to avoid its previously detected limitations. The article describes in detail these limitations and their corresponding proposed improvements. The validation of the proposed solution was carried out using the Lyapunov Criterion to demonstrate the stability of this approach. Some experiments were implemented in a simulation environment using MATLAB. These experiments show significant improvement of the proposed control law in comparison with the existing control law. Finally, the validation of the proposed control law was carried out in a Platform in the laboratory with a real robot. The results of these experiences showed results similar to the obtained in simulation time, which indicates that these results are consistent and promising. Future work includes the relation of the proposed solution with other kinds of approaches such as obstacles avoidance, trajectory tracking, path following, simultaneous mapping, and multi-agent systems.

REFERENCES

[1] W. A. Gruver, "Intelligent robotics in manufacturing, service, and rehabilitation: An overview," *IEEE Trans. Ind. Electron.*, vol. 41, no. 1, pp. 4–11, 1994.
[2] M. O. Qureshi and R. S. Syed, "The impact of robotics on employment and motivation of employees in the service sector, with special reference to health care," *Saf. Health Work*, vol. 5, no. 4, pp. 198–202, 2014.
[3] A. G. Ozkil, Z. Fan, S. Dawids, H. Aanes, J. K. Kristensen, and K. H. Christensen, "Service robots for hospitals: A case study of transportation tasks in a hospital," in *Conf. Autom. Logist.*, pp. 289–294, 2009.
[4] S. Jeon and J. Lee, "Performance analysis of scheduling multiple robots for hospital logistics," in *14^{th} Int. Conf. Ubiquitous Robot. Ambient Intel.*, pp. 937–940, 2017.
[5] M. Guinaldo, E. Fábregas, G. Farias, S. Dormido-Canto, D. Chaos, J. Sánchez, and S. Dormido, "A mobile robots experimental environment with event-based wireless communication," *Sens.*, vol. 13, no. 7, pp. 9396–9413, 2013.
[6] G. Farias, E. Fabregas, E. Peralta, E. Torres, and S. Dormido, "A Khepera IV library for robotic control education using V-REP," *IFAC-PapersOnLine*, vol. 50, no. 1, pp. 9150 – 9155, 2017, 20^{th} IFAC World Congress.
[7] T. Samad and A. Annaswamy, "Success stories for control: Mobile-robot-enabled smart warehouses," *Impact Control Technol.*, pp. 1–2, 2011.
[8] P. Ganesan, G. Sajiv, and L. M. Leo, "Warehouse management system using microprocessor based mobile robotic approach," in *3^{rd} Inter. Conf. Sci. Technol. Eng. Manag.*, pp. 868–872, 2017.
[9] A. M. Bloch, M. Reyhanoglu, and N. H. McClamroch, "Control and stabilization of nonholonomic dynamic systems," *IEEE Trans. Autom. Control*, vol. 37, no. 11, pp. 1746–1757, Nov. 1992.
[10] C. de Wit and O. Sordalen, "Exponential stabilization of mobile robots with nonholonomic constraints," *IEEE Trans. Autom. Control*, vol. 37, no. 11, pp. 1791–1797, 1992.
[11] A. Widyotriatmo and K.-S. Hong, "Navigation function-based control of multiple wheeled vehicles," *IEEE Trans. Ind. Electron.*, vol. 58, no. 5, pp. 1896–1906, 2011.
[12] X. Yu and L. Liu, "Distributed formation control of nonholonomic vehicles subject to velocity constraints," *IEEE Trans. Ind. Electron.*, vol. 63, no. 2, pp. 1289–1298, 2016.
[13] C. C. de Wit, B. Siciliano, and G. Bastin, *Theory of robot control*. Springer, 1996.
[14] C. C. de Wit, B. Siciliano, and G. Bastin, *Theory of robot control*. Springer Science & Business Media, 2012.
[15] R. Siegwart, I. R. Nourbakhsh, and D. Scaramuzza, *Introduction to autonomous mobile robots*. MIT press, 2011.
[16] S. K. Malu and J. Majumdar, "Kinematics, localization and control of differential drive mobile robot," *Glob. J. Res. Eng.*, 2014.
[17] F. Pourboghrat and M. P. Karlsson, "Adaptive control of dynamic mobile robots with nonholonomic constraints," *Comput. Electr. Eng.*, vol. 28, no. 4, pp. 241 – 253, 2002.
[18] Y. Koren and J. Borenstein, "Potential field methods and their inherent limitations for mobile robot navigation," in *IEEE Int. Conf. Robot. Autom.*, pp. 1398–1404, 1991.
[19] V. J. G. Villela, R. Parkin, M. L. Parra, J. M. D. González, M. J. G. Liho, and H. Way, "A wheeled mobile robot with obstacle avoidance capability," *Tecnología Y Desarrollo*, vol. 1, no. 5, pp. 159–166, 2004.
[20] O. Khatib, "Real-time obstacle avoidance for manipulators and mobile robots," in *Autonomous robot vehicles*, pp. 396–404. Springer, 1986.
[21] E. Fabregas, G. Farias, E. Peralta, H. Vargas, and S. Dormido, "Teaching control in mobile robotics with V-REP and a Khepera IV library," in *IEEE Conf. Control Appl.*, pp. 821–826, 2016.
[22] E. Peralta, E. Fabregas, G. Farias, H. Vargas, and S. Dormido, "Development of a Khepera IV library for the V-REP simulator," *IFAC-PapersOnLine*, vol. 49, no. 6, pp. 81–86, 2016, 11^{th} IFAC Symposium on Advances in Control Education.
[23] E. Fabregas, G. Farias, S. Dormido-Canto, M. Guinaldo, J. Sánchez, and S. Dormido, "Platform for teaching mobile robotics," *J. Intel. Robot. Syst.*, vol. 81, no. 1, pp. 131–143, 2016.

[24] F. Kühne, W. F. Lages, and J. M. G. da Silva Jr, "Point stabilization of mobile robots with nonlinear model predictive control," in *IEEE Int. Conf. Mechatron. Autom.*, vol. 3, 2005.
[25] D. Galán, E. Fabregas, G. Garcia, J. Sáenz, G. Farias, S. Dormido-Canto, and S. Dormido, "Online virtual control laboratory of mobile robots," *IFAC-PapersOnLine*, vol. 51, no. 4, pp. 316–321, 2018, 3^{rd} IFAC Conference on Advances in Proportional-Integral-Derivative Control.
[26] C. Samson, "Time-varying feedback stabilization of car-like wheeled mobile robots," *Int. J. Robot. Res.*, vol. 12, no. 1, pp. 55–64, 1993.
[27] Y. Ma, V. Cocquempot, M. E. B. El Najjar, and B. Jiang, "Actuator failure compensation for two linked 2wd mobile robots based on multiple-model control," *Int. J. Appl. Math. Comput. Sci.*, vol. 27, no. 4, pp. 763–776, 2017.
[28] T. Lozano-Perez, *Autonomous robot vehicles*. Springer Science & Business Media, 2012.
[29] Y. Kanayama, Y. Kimura, F. Miyazaki, and T. Noguchi, "A stable tracking control method for an autonomous mobile robot," in *IEEE Int. Conf. Robot. Autom.*, pp. 384–389, 1990.
[30] K. Kozłowski, *Robot Motion and Control 2009*. Springer, 2009.
[31] J. M. Godhavn and O. Egeland, "Lyapunov-based time varying control for exponential stabilization of a unicycle," *IFAC Proc. Vol.*, vol. 29, no. 1, pp. 2454–2459, 1996.
[32] L. Jie and Z. Wei, "Posture stabilization of kinematic model of differential drive robots via lyapunov-based control design," *World Acad. Sci. Eng. Technol. Int. J. Mech. Aerosp. Ind. Mechatron. Manuf. Eng.*, vol. 10, no. 8, pp. 1587–1592, 2016.
[33] H. K. Khalil, *Nonlinear systems (3^{rd} ed.)*. Prentice Hall, 2002.
[34] R. W. Brockett *et al.*, "Asymptotic stability and feedback stabilization," *Differ. Geom. Control Theory*, vol. 27, no. 1, pp. 181–191, 1983.
[35] G. Farias, E. Fabregas, E. Peralta, H. Vargas, S. Dormido-Canto, and S. Dormido, "Development of an easy-to-use multi-agent platform for teaching mobile robotics," *IEEE Access*, vol. 7, no. 1, pp. 55 885–55 897, 2019.

Ernesto Aranda-Escolástico received the M.S. degree in physics from the Complutense University of Madrid, Spain, in 2013, and the M.S. degree in control engineering from National Distance Education University (UNED), Spain, in 2014. He obtained the Ph.D. in computer science from the UNED in 2018. Currently he is working at the Department of Informatics, ceiA3, CIESOL, University of Almería. His research interests include event-triggered control, networked control systems, multi-rate systems, and nonlinear systems.

Gonzalo Garcia received a BS in Electronics Engineering with a major in Radar Design from the Chilean Naval Polytechnic Academy, 1994, a MS in Electronics Engineering with a major in Automatic Control, from the Universidad Tecnica Federico Santa Maria, Valparaiso, Chile, 2006, and a PhD in Aerospace Engineering, from the University of Kansas, 2013. Currently he is Postdoctoral Fellow at the Department of Ocean and Mechanical Engineering, Florida Atlantic University (FAU). His research and teaching activities are related with the design of advanced flight control systems for unmanned aerial vehicles, robust control, nonlinear control, optimal control, and predictive control.

Ernesto Fabregas received a B.S. in automation and an M.S. in digital systems from the Polytechnic University "Jose Antonio Echeverría" (CUJAE), Havana, Cuba, in 2004 and 2008, respectively, and a Ph.D. in computer science from the Universidad Nacional de Educación a Distancia (UNED), Madrid, Spain, in 2013. Currently he is Postdoctoral Fellow in the UNED. His current research interests include simulation and control of pattern recognition, machine learning, multi-agent systems, mobile robot control.

Dictino Chaos received the B.D. in Physics from the Complutense University of Madrid in 2004, and Ph.D. in Computer Engineering and Automatic Control in 2010 from UNED awarded with a special prize for the best Thesis. Currently, he holds an Associate Professor position with the Department of Computer Science and Automatic Control UNED. His research interests include nonlinear control, tracking, point stabilization, and path following of under-actuated vehicles, the stability of switched systems, machine vision, and robotics.

Gonzalo Farias received the degree in computers science from the De la Frontera University, Temuco, Chile, in 2001 and the PhD degree in computer science from the National University of Distance Education (UNED), Madrid, Spain, in 2010. Since 2012, he has been with the Electrical Engineering School at Pontificia Universidad Católica de Valparaíso (PUCV). His current research interests include machine learning, pattern recognition, simulation and control of dynamic system and engineering education.

Sebastián. Dormido-Canto received the M.S. degree in electronics engineering from the Universidad Pontificia de Comillas (ICAI), Madrid, Spain, in 1994 and the Ph.D. degree in physics from the Universidad Nacional de Educación a Distancia (UNED), Madrid, in 2001. Since 1994, he has been with the Department of Computer Science and Automatic Control, UNED, where he is currently a Full Professor of control engineering. His research and teaching activities are related with the pattern recognition, machine learning, parallel processing and nuclear fusion.

Sebastián Dormido Bencomo Sebastián Dormido received the B.S. degree in physics from Complutense University (UCM), Madrid, Spain, in 1968, the Ph.D. degree in the sciencegs from Basque Country University, Bilbao, Spain, in 1971, and the Doctor Honorary degree from the Universidad de Huelva and the Universidad de Almería. In 1981, he was appointed as a Professor of Control Engineering with the National University of Distance Education, Madrid. He has authored or co-authored over 250 technical papers in international journals and conferences, and has supervised over 35 Ph.D. theses. His scientific activities include computer control of industrial processes, model-based predictive control, hybrid control, and Web-based laboratories for distance education. From 2001 to 2006, he was the President of the Spanish Association of Automatic Control, CEA-IFAC. He has received the National Automatic Control Prize from the IFAC Spanish Automatic Control Committee. Currently he is Emeritus Professor at UNED.